Portable X-ray fluorescence to optimize stream sediment chemistry and indicator mineral surveys, case 1: Carbonatite-hosted Nb deposits, Aley carbonatite, British Columbia, Canada

Duncan A.R. Mackay[1] and George J. Simandl[1, 2, a]

[1] University of Victoria, School of Earth and Ocean Sciences, Victoria, BC, V8P 5C2
[2] British Columbia Geological Survey, Ministry of Energy and Mines, Victoria, BC, V8W 9N3
[a] corresponding author: George.Simandl@gov.bc.ca

Recommended citation: Mackay, D.A.R., and Simandl, G.J., 2014. Portable X-ray fluorescence to optimize stream sediment chemistry and indicator mineral surveys, case 1: Carbonatite-hosted Nb deposits, Aley carbonatite, British Columbia, Canada. In: Geological Fieldwork 2013, British Columbia Ministry of Energy and Mines, British Columbia Geological Survey Paper 2014-1, pp. 183-194.

Abstract

The Aley carbonatite-hosted deposit is the most important Nb resource in the British Columbia alkaline province. Portable X-ray fluorescence (pXRF) was used effectively to determine concentrations of carbonatite pathfinder elements (Nb, Ta, La, Ce, Pr, Nd, Y, Th, U, Ba, and Sr) in stream sediments. Investigation of sediments of the unnamed creek ("Al creek") draining the Aley carbonatite area, indicates that the + 250 µm, + 125 µm, and + 63 µm size fractions contain high concentrations of carbonatite pathfinder elements (Nb, Ta, La, Ce, Pr, Nd, U, and Th) relative to other size fractions. The + 125 µm fraction was chosen for systematic evaluation of the pathfinder element distribution in Al Creek sediments because it is suitable for chemical analysis and Quantitative Evaluation of Materials by Scanning electron microscopy (QEMSCAN). This method will be used in the second part of this study, which will concentrate on indicator minerals. The same samples enriched in pathfinder elements are expected to contain minerals characteristic of carbonatites such as pyrochlore, columbite-(Fe), fersmite, monazite-(Ce), rare earth element (REE)-bearing fluorocarbonates, barite, and apatite. As expected, samples overlying the deposit and immediately downstream from the Aley carbonatite have the highest concentrations of pathfinder elements. Optical microscopy, electron microprobe (EMP), laser ablation inductively coupled plasma mass spectrometry (LA-ICP-MS), and QEMSCAN studies of these samples are required to identify the most useful carbonatite indicator minerals and quantify their relative abundances with increasing distance from the deposit.

Keywords: Niobium, tantalum, indicator minerals, pathfinder elements, stream sediment, carbonatite, portable x-ray fluorescence, pyrochlore, fersmite, columbite

1. Introduction

Carbonatites, carbonatite complexes, and their weathered equivalents are the main sources of Nb (Mariano, 1989a, b; Birkett and Simandl, 1999; Simandl et al., 2012, 2013a; Tantalum-Niobium International Study Center, 2013). They are most common along rift zones in intracratonic settings (Woolley and Kjarsgaard, 2008). The Aley carbonatite is one of a series of carbonatite complexes, syenite complexes, and other alkaline rocks that forms the British Columbia alkaline province (Fig. 1; Pell, 1994). It lies 135 kilometres north of Mackenzie, British Columbia and 20 kilometres northeast of the Ospika Arm of Williston Lake, east of the Rocky Mountain Trench (Fig. 1) and was discovered following base metal exploration (Pride, 1983). It was the subject of further study and exploration over the next 30 years (Mäder, 1986, 1987; Pride, 1987a, b; Robert et al., 2005; Nethery, 2007; Chung and Crozier, 2008). The deposit has a measured resource of 113 million tonnes at 0.41% Nb_2O_5 and an indicated resource of 173 million tonnes at 0.35% Nb_2O_5 with a cutoff grade of 0.20% Nb_2O_5 (Taseko Mines Limited, 2013).

The main objectives of this study are to: 1) determine if stream sediment geochemistry can be used effectively to explore for Aley-type deposits; 2) establish the best stream sediment size fraction for indicator minerals that might point to Nb-bearing carbonatite deposits; 3) characterize the geochemical gradient of potential pathfinder elements (Nb, Ta, REEs, P, Ba, Sr, U, and Th) in sediments downstream from the deposit; and 4) evaluate the usefulness of pXRF analyses for preliminary assessment of indicator mineral and stream sediment studies.

2. Geological setting

Rocks of the British Columbia alkaline province were emplaced during three main events: ~ 800-700 Ma (postulated breakup of Rodinia), ~ 500 Ma (extensional tectonism and attenuation of the continental margin), and ~ 360-340 Ma (renewed extensional tectonics; Pell, 1994; Millonig et al., 2012). Multiple phases of deformation and associated sub-greenschist to amphibolite grade metamorphism overprinted the carbonatites between ~ 155 and 50 Ma (Pell, 1994; Millonig et al., 2012).

The Aley carbonatite cuts Lower to Middle Paleozoic sedimentary rocks of the western Cordilleran foreland fold and thrust belt (Figs. 1, 2). The regional geology of the area was originally mapped at the scale of 1:253,440 by Irish (1970). The deposit is in the Cassiar terrane, which includes a platformal assemblage of siliciclastic and carbonate rocks

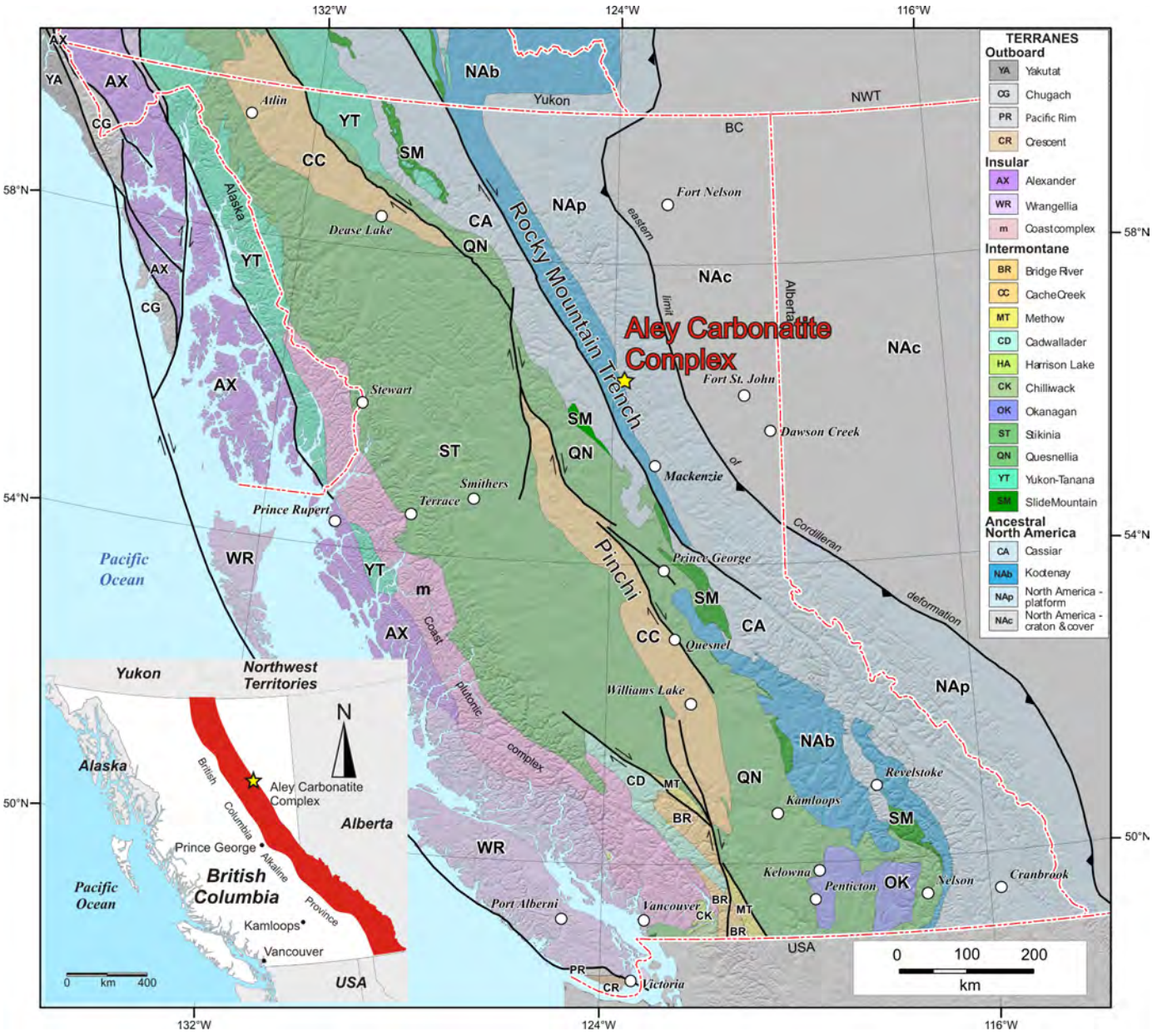

Fig. 1. Tectonic setting of the Aley carbonatite complex (yellow star). British Columbia alkaline province shown in red (inset map). Municipalities are denoted by white circles. Modified after Pell (1994).

that were deposited along the western margin of Laurentia (Mäder, 1986; Pell, 1994). The Kechika Formation (Cambrian to Early Ordovician) unconformably overlies the Rosella Formation (Lower Cambrian; Pyle and Barnes, 2001). It consists of argillaceous limestone, calcareous siltstone, and dolostone. The Skoki Formation (Lower to Middle Ordovician) is generally in fault contact with the Kechika Formation and consists of dolostone and volcanic rocks (Mäder, 1986). The Road River Group (Lower to Upper Ordovician-Silurian) caps the succession, locally unconformably overlies the Skoki Formation, and consists of cherty dolostone, shale, argillaceous limestone, and rare quartzite and quartz pebble conglomerate (Mäder, 1986; Pyle and Barnes, 2001). Regional metamorphism reached lower greenschist facies (Mäder, 1986) and coincided with convergent tectonism and orogenesis between ~ 155 and 50 Ma (Pell, 1994; Millonig et al., 2012).

The metasedimentary sequence was intruded by the Aley carbonatite, REE-bearing carbonatite dikes, the Ospika diatreme, and lamprophyre dikes (Fig. 2; Mäder, 1986; Pell, 1994; McLeish, 2013). Zircon from the dolomite carbonatite phase of the Aley carbonatite contains insufficient radiogenic Pb for U-Pb geochronology (Mäder, 1986; McLeish, 2013), but McLeish (2013) reported a U-Pb titanite age of 365.9 ± 2.1 Ma for the Ospika diatreme. The Aley carbonatite displays an early phase of deformation lacking in the Ospika diatreme indicating that it is older than ~ 366 Ma (McLeish, 2013). The Road River Group, (Lower to Upper Ordovician-Silurian, based on conodont biostratigraphy; Mäder, 1986; Pyle and

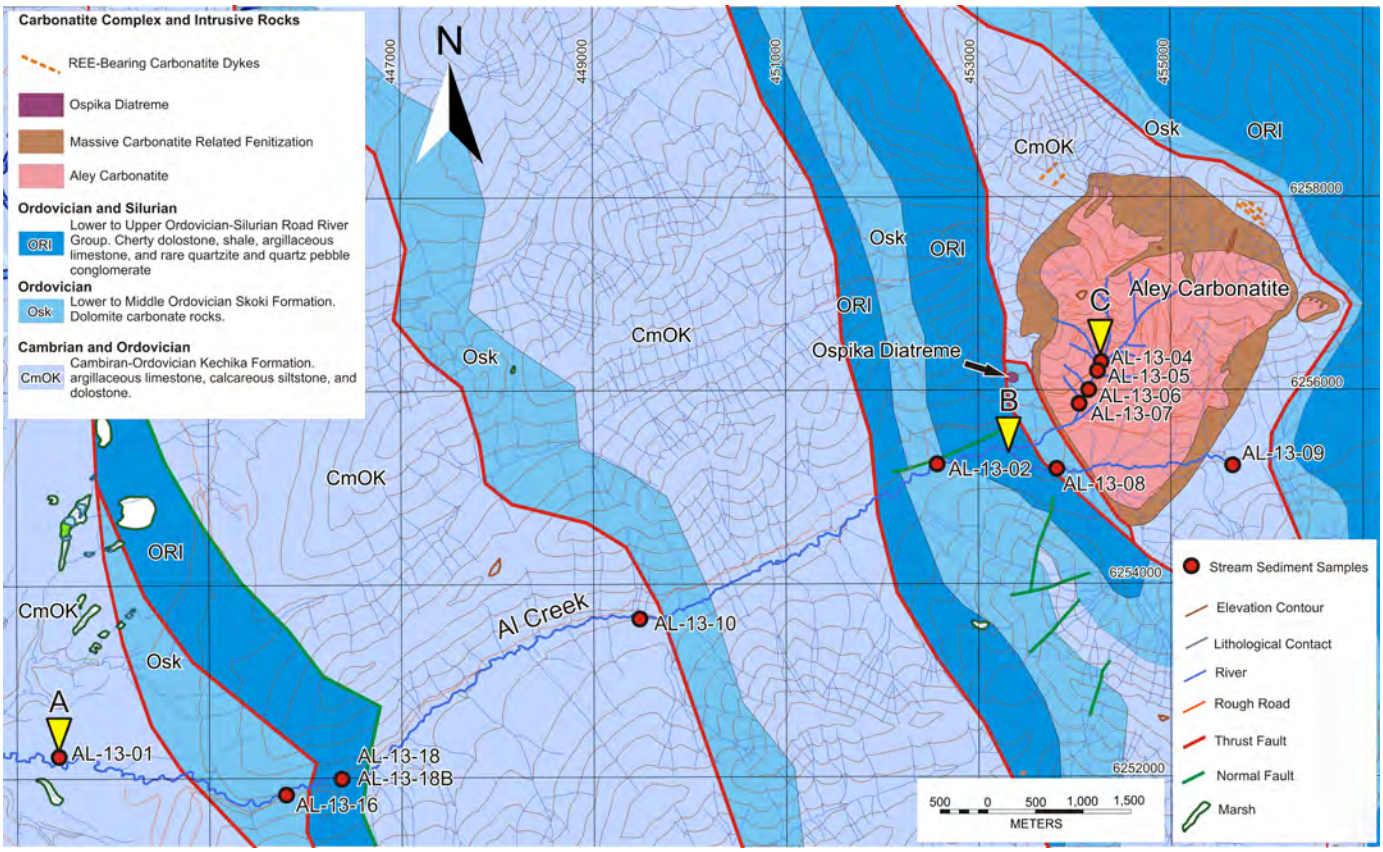

Fig. 2. Geological setting of the Aley carbonatite and locations of stream sediment samples. Yellow markers (A-B-C) denote location of profile in Figure 6. Modified after Pride (1983), Mäder (1986), Massey et al. (2005), and McLeish (2013). UTM zone 10, NAD 83.

Barnes, 2001), is the youngest unit overprinted by this early deformation that is cut by lamprophyre dikes (considered related to the Aley carbonatite and Ospika diatreme) suggesting that the Aley carbonatite is older than 366 Ma and younger than the Road River Group (McLeish, 2013).

3. Geology of the Aley carbonatite complex

The Aley carbonatite outcrops intermittently over an area 3 to 3.5 km in diameter (Fig. 2; Mäder, 1986). It intruded sedimentary host rocks as a sill and was subsequently folded within a recumbent nappe (McLeish et al., 2010; McLeish. 2013). The main phase of the carbonatite consists of layered or banded dolomite carbonatite surrounded by minor calcite carbonatite (Mäder, 1986). Kressal et al. (2010) observed that the dolomite carbonatite phase contains apatite, pyrite, calcite, and Nb-bearing minerals such as fersmite [(Ca,Ce,Na)(Nb,Ta,Ti)$_2$(O,OH,F)$_6$], pyrochlore [(Na,Ca)$_2$Nb$_2$O$_6$(OH,F)], columbite-(Fe) [(Fe,Mn)Nb$_2$O$_6$] and rare, fine-grained acicular aggregates of Nb-rich rutile [(Ti, Nb, Fe)O$_2$]. Pods or lenses of magnetite (10s of centimetres to metres in size) are found throughout the dolomite carbonatite phase and contain apatite, phlogopite, Nb-bearing minerals, zircon, and interstitial carbonates (Kressall et al., 2010). The magnetite pods likely represent deformed and distended cumulate layers (Kressall et al., 2010). Monazite commonly co-exists with fersmite in pseudomorphs after primary columbite-(Fe) or pyrochlore (Mäder, 1986; Kressall et al., 2010).

Massive fenite surrounds the carbonatite intrusion (Fig. 2). It displays a characteristic dark blue-green colour and contains abundant richterite, arfvedsonite, and aegirine (Mäder, 1986; Kressall et al., 2010). The fenite contains brecciated metasedimentary and feldspathic material. The feldspathic breccia clasts resemble altered syenite fragments; however, they are probably strongly fenitised and albitised fragments of the Kechika Formation.

Carbonatite dikes exposed on the northwest ridge above the main deposit (Fig. 2) contain significant concentrations of light rare earth elements (LREE; Mäder, 1986). The LREE mineralisation consists of REE-bearing carbonates and fluorocarbonates (Mäder, 1986). The dikes probably represent late differentiated phases of the Aley carbonatite melt (Mäder, 1986).

4. Methods

4.1. Sample collection

Twelve stream sediment samples were collected from a creek ("Al", Fig. 2) draining the Aley carbonatite during the 2013 field season (Table 1). One sample was collected upstream of the deposit to assess background geochemistry. Four samples, spaced 200 to 300 m apart, were collected along

Fig. 3. Al-13-05 sample site; dry pool below chute over fenite bedrock. Sampled material forms matrix between cobbles and boulders. Looking north up the dry stream bed valley toward the Aley Carbonatite. Shovel is 1 m long.

the dry tributary of Al Creek directly over the deposit (Fig. 3). The remaining seven samples were collected along the creek, downstream from the deposit, 1.5 to 3 km apart as access allowed (Figs. 2, 4). The bed of the creek consists mainly of boulders, cobbles, and pebbles (Fig. 4). Sample sites included dry pools (Fig. 3), and the lee areas of boulders and fallen trees, and bars (Table 1). Matrix material between cobbles and boulders, generally from an area < 1 m^2, was sampled (Fig. 4; Table 1). Organic material (conifer needles, leaves, and twigs) was scrapped from the surface of samples sites. Not all of the organic material could be avoided during sample collection, and minor amounts were retained in the coarser fractions (+ 500 µm and coarser). Material was wet sieved through a + 8 mm screen, except where noted in Table 1. Weights for dried samples range from 4.1 to 21.8 kg. Sample AL-13-18B is a pre-concentrate (washed by hand using a pan) of stream sediment close to sample AL-13-18.

Fig. 4. Al-13-08 sample site; Al creek, downstream of the Aley carbonatite. Sampled material constitutes matrix between cobbles and boulders, which form the predominant substrate. Stream is 3.5 m wide; looking east upstream.

4.2. Sample preparation and portable XRF analyses

Samples were dried in an oven at 40°C, weighed, and dry sieved into + 4 mm, 2 mm to 4 mm, 1 mm to 2 mm, 500 µm to 1 mm, 250 µm to 500 µm, 125 µm to 250 µm, 63 µm to 125 µm, and - 63 µm fractions. To shorten the text and simplify figures, the following notation was used throughout for the same grain size intervals; + 4 mm, + 2 mm, + 1 mm, + 500 µm, + 250 µm, + 125 µm, + 63 µm, and - 63 µm. Each size fraction was weighed individually. Selected size fractions were split using a riffle splitter with a portion being kept as a witness sample, a portion for magnetic separation, and a portion for XRF analyses. Samples for XRF analyses were milled using ring and roller bowl tungsten carbide mills. Standard XRF sample pulp cups were then prepared and analysed by portable XRF. Analyses were carried out using a portable Thermo Fisher Scientific Niton FXL-950 instrument. A complete description of equipment, specifications, sample preparation, and laboratory methods and information about standards, operating procedures, instrument settings, limits of detections, and data quality control are in Luck and Simandl (2014).

The factory-calibrated pXRF data are internally consistent and have acceptable precision; however, they were not recalibrated using results of standard laboratory analyses [lithium metaborate inductively couple plasma mass spectrometry (LMB ICP-MS)] as described in Simandl et al. (2013b) to improve accuracy by correcting for matrix effects and analytical bias. For example, good accuracy is expected for La and Nb. Other elements (e.g. Sr) are underestimated.

Table 1. Characteristics of stream channel and sample sites. Sample AL-13-09 was collected upstream of the deposit. Samples Al-13-04, AL-13-05, AL-13-06, and AL-13-07 were collected directly over the deposit. Remaining samples are in order of increasing distance downstream of the deposit.

	Location		Elevation	Stream Character			Clast Size (cm)		Dry wt.	Sample Site Characteristics
Sample ID	Northing	Easting	(m)	Width (m)	Depth (m)	Flow	Average	Maximum	(kg)	
AL1309	6255259	455696	1406	2.5	0.2	moderate	2 to 5	30	14.2	Lee of fallen tree; clasts predominantly white dolomite, limestone, and slate.
AL1304	6256338	454355	1520	1.5	N/A	N/A	2 to 5	50	4.9	Exposed bedrock (partly covered by boulders); dry streambed; sampled from matrix between cobbles and boulders; not sieved in the field.
AL1305	6256192	454249	1479	3	N/A	N/A	5 to 10	40	6.7	Dry pool below chute in dry streambed (Fig. 3); exposed bedrock (partly covered by boulders); not sieved in the field.
AL1306	6256016	454132	1431	2	N/A	N/A	3 to 5	150	6.8	Fine-grained material in dry pools (< 50 x 50 cm) between fenite and carbonatite cobbles and boulders; not sieved.
AL1307	6255865	454059	1400	2	N/A	N/A	2 to 5	35	6.9	Dry pool below cobbles and boulders; no exposed bedrock in dry streambed; large skree slope upstream; not sieved.
AL1308	6255181	453823	1298	3.5	0.3	rapid	5 to 15	100	9.4	Sample from matrix between cobbles and boulders (Fig. 4); predominantly slate and limestone clasts; rare fenite breccia clasts.
AL1302	6255244	452580	1246	3.5	0.3	rapid	5 to 10	150	14.7	Sample from matrix between cobbles and boulders; rare fenite boulders
AL1310	6253666	449483	1082	4.5	0.4	rapid	5 to 10	200	14.8	Near stream bank in active channel; lee of boulders; upstream of several slides; slate, limestone, and rare fenite breccia clasts are predominant.
AL1318	6251991	446312	928	4	0.8	rapid	1 to 2	200	12.2	Bar (4 x 16 m) downstream of fallen trees; sample from matrix between pebbles and cobbles; downstream of several slides; few subrounded to subangular fenite, carbonatite, and Ospika diatreme boulders a few m downstream of sample site.
AL1318B	6251991	446314	928	4	0.8	rapid	1 to 2	200	4.1	Same as above; preconcetrate (seived to 8 mm then washed in pan) sample close to AL-13-18.
AL1316	6251818	445779	891	3	0.4	rapid	2 to 5	40	14.4	5 x 10 m area in lee of fallen trees; upstream of a landslide.
AL1301	6252228	443432	793	5	0.3	rapid	1 to 3	15	21.8	Lee of fallen trees.

Remaining elements, including U and Th, are overestimated. Based on strong positive correlation between 11 U and 15 Th pXRF, and corresponding LMB-ICPMS analyses of stream sediments from Aley, Lonnie and Wicheeda (unpublished) processed in exactly the same manner as those in the present study, U and Th are overestimated of the order of 35% and 90% respectively. The pXRF is not a substitute for traditional laboratory methods where high accuracy and precision are required.

5. Results

Samples AL-13-02, AL-13-18, and AL-13-18B, were chosen for systematic study of all size fractions. The particle size distributions for samples AL-13-02 and AL-13-18 are skewed toward coarser size fractions, whereas AL-13-18B displays a nearly normal distribution (Fig. 5).

In samples Al-13-18 and Al-13-18B, Nb, Ta, Y, La, Ce, Pr, Nd, U, Th, and P are enriched in the + 125 µm, and + 63 µm size fractions relative to other sizes (Fig. 5). Similar trends exist for Al-13-02, however, the + 250 µm, and + 500 µm fractions also contain relatively high Nb, Ta, Y, La, Ce, Pr, Nd, U, and Th concentrations. Phosphorus is detectable in the + 125 µm fraction for AL-13-18 and AL-13-18B, but is below the limit of detection in the + 125 µm fraction for sample AL-13-02. High abundances of pathfinder elements (relative to other size fractions from the same samples) are also observed in the + 125 µm and + 63 µm size fractions in sediments from the nearby Lonnie (Luck and Simandl, 2014) and Wicheeda (Mackay and Simandl, 2014) carbonatite study areas. The + 125 µm fraction was chosen for systematic study because of these higher abundances and because it is a suitable size for indicator mineral studies.

The ranges in abundance of selected major oxides (Table 2) are: < 16.5 to 45.8 wt% SiO_2, < 1.8 to 7.0 wt% Al_2O_3, 1.3 to 15.2 wt% Fe_2O_3, 10.9 to 31.8 wt% CaO, < 0.1 to 0.3 wt% TiO_2, < 1.4 to 6.4 wt% MgO, and 0.2 to 2.6 wt% K_2O. Concentration ranges for trace elements (Table 2) are: 15 to 9988 ppm Nb, < 7 to 166 ppm Ta, 14 to 170 ppm Y, 70 to 2010 ppm La, 115 to 2977 ppm Ce, 147 to 1579 ppm Nd, 80 to 661 ppm Pr, 140 to 910 ppm Ba, 177 to 2018 ppm Sr, < 90 to 9412 ppm P, < 1 to 62 ppm U, and 9 to 570 ppm Th.

6. Discussion

High concentrations of Nb, Ta, La, Ce, Pr, Nd, U, and Th in the + 250 µm, + 125 µm, and + 63 µm fractions (Fig. 5) probably reflect the presence of carbonatite indicator minerals. The highest values typically coincide with the Aley carbonatite (samples AL-13-04, AL-13-05, AL-13-06; Figs. 6, 7). As expected, relative concentrations as high as 9988 ppm Nb, 133 ppm Ta, 2010 ppm La, 2977 ppm Ce, 171 ppm Y, 44 ppm U, 570 ppm Th, and 2018 ppm Sr occur over or directly downstream of the deposit and decrease with increasing distance downstream to between 3495 and 3311 ppm Nb, 79 and 73 ppm Ta, 596 and 561 ppm La, 936 and 866 ppm Ce, 72 and 71 ppm Y, 35 and 26 ppm U, 266 and 251 ppm Th, and 827 and 711 ppm Sr (Figs. 6, 7; Table 2). Barium does not follow this trend, suggesting barite input from dolostones and argillaceous limestones of the Skoki and Kechika formations.

Samples taken immediately below slides (greater than 200 m^2) and scree slopes (such as AL-13-07) show a decrease in the concentrations of Nb, Ta, La, Ce, Y, U, Th, and Sr relative to adjacent upstream (Al-13-06) and downstream samples (AL-13-02; Figs. 6, 7). This demonstrates the effect of dilution of pathfinder elements by incorporation of unmineralized material (unconsolidated overburden and slate and limestone scree). Sample AL-13-02, taken in an active stream channel, has higher concentrations of pathfinder elements relative to AL-13-07 (Fig. 6), possibly due to concentration of indicator minerals by winnowing. Sample AL-13-09, obtained upstream of the Aley carbonatite (Fig. 7), has low concentrations of carbonatite pathfinder elements relative to samples downstream of the deposit. Subrounded to subangular carbonatite, fenite, and diatreme boulders were found immediately downstream of AL-13-18 and AL-13-18B (Figs. 6, 7; Table 2). It is unclear if these boulders were derived from the Aley carbonatite or a different occurrence. Sample AL-13-16, downstream of this site, displays an increase in Nb, Ta, La, Ce, Y, U, Th, and Ba relative to Al-13-18 and AL-13-18B, which may be related to the boulders.

High coefficients of determination for pathfinder elements (Fig. 8) probably represent indicator mineral chemistry and mineral assemblages. The strong linear dependence between Nb and Fe_2O_3 ($R^2 = 0.97$; Fig. 8a) likely represents the co-occurrence of Nb-bearing minerals and magnetite in the stream sediments. Correlation between Nb and Ta ($R^2 = 0.83$; Fig. 8b) agrees with the expected presence of pyrochlore, columbite-(Fe), and/or fersmite in the stream sediments. The Nb:Ta ratio of pyrochlore and columbite-(Fe) from carbonatites is typically high and is reflected in the high (on average 50:1) Nb:Ta ratio of the sediments (Table 2). Niobium and La ($R^2 = 0.81$; Fig. 8c) display a strong relationship which is likely the result of coincidence of Nb-bearing and REE-bearing minerals in the stream sediments. It remains unclear if most of the REEs are in the crystal structure of Nb-bearing minerals rather than REE-bearing carbonates, fluorocarbonates, and/or phosphates. Poor linear dependence between Nb and TiO_2 ($R^2 = 0.20$; Fig. 8d) is likely the result of low Ti concentrations expected in pyrochlore sourced from carbonatites. It may also indicate negligible concentrations of Nb-rutile in stream sediments, mirroring the low abundances in the deposit reported by Kressal et al. (2010). Samples AL-13-04, AL-13-05, and AL-13-06 have the highest Nb contents (Fig. 7 a-d) and fail to plot directly on the best-fit line (Fig. 8a). These samples were taken from a dry tributary of Al creek; the higher Nb contents might reflect reduced levels of fluvial reworking in an intermittent stream. Alternatively, they might be the consequence of local variations in the concentration of fersmite, columbite, and pyrochlore in underlying mineralisation.

Cerium correlates strongly with La ($R^2 = 0.99$) and well with Nd ($R^2 = 0.95$), Pr ($R^2 = 0.94$), and Y ($R^2 = 0.85$). This

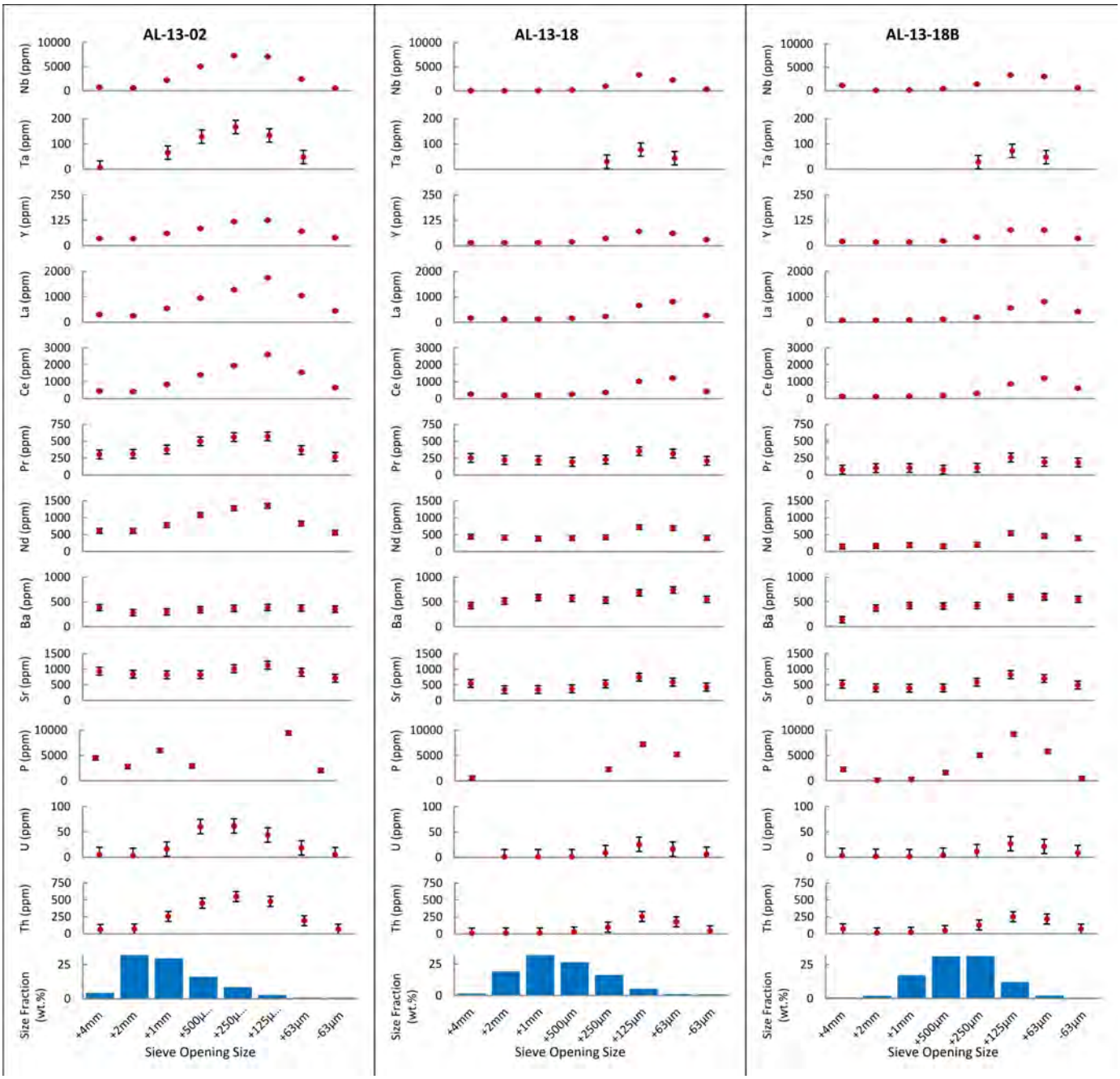

Fig. 5. Portable XRF analyses for selected trace elements and grain size fraction distributions of samples AL-13-02, AL-13-18, and AL-13-18B. The + 250 µm, + 125 µm, and + 63 µm size fractions are enriched in Nb, Ta, Y, La, Ce, Pr, Nd, P, U, and Th relative to other size fractions. Analyses below detection limits are not shown. Error bars based on average 2σ values determined from multiple analyses of standards by pXRF (Luck and Simandl, 2014).

is expected because REEs have similar physical and chemical properties and commonly substitute for each other in monazite, REE-bearing carbonates and fluorocarbonates, and Nb-bearing minerals. Strong correlation between Ce and Th ($R^2 = 0.90$) may reflect accumulations of monazite. Zirconium correlates well with Ce ($R^2 = 0.95$), Nd ($R^2 = 0.88$), and Pr ($R^2 = 0.87$), La ($R^2 = 0.86$), and Y ($R^2 = 0.82$) and may relate to concentrations of zircon and co-occurrence with REE-bearing minerals. As expected, a significant relationship exists between Th and U concentrations ($R^2 = 0.70$).

An unknown analytical error may explain < 90 ppm P values for samples collected from directly over the deposit (Figs. 6, 7), which contains local apatite (2-10%, Kressall et al. 2010). As P is a light element; it has to be present in high concentrations to be a useful pathfinder due to error induced by the matrix effects of Ca and Fe (Simandl et al., 2013b).

Lack of linear dependence between Sr and Ba ($R^2 = 0.06$) suggest that these elements are not present as a uniform barite-

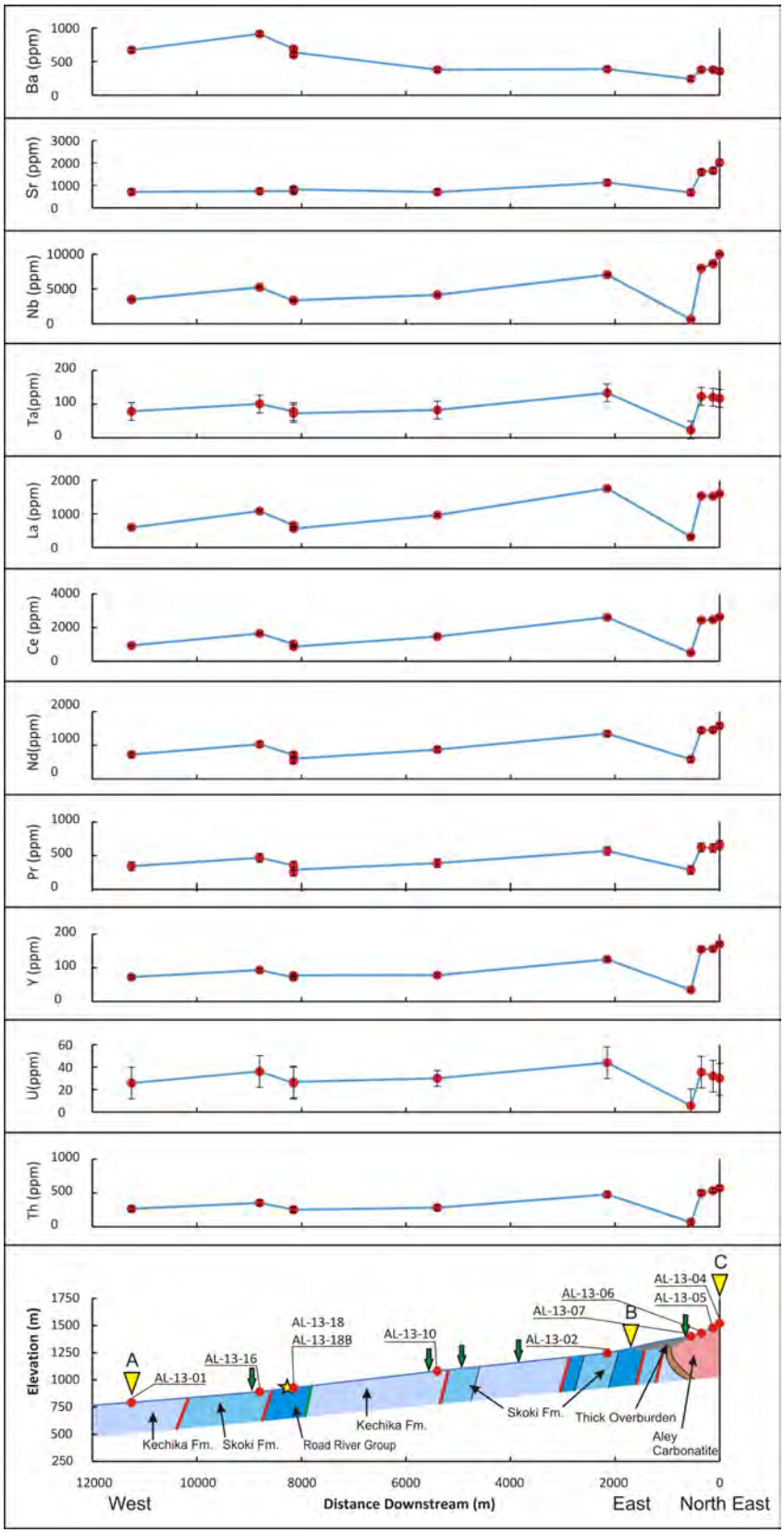

Fig. 6. Downstream variation in carbonatite pathfinder elements concentrations (+ 125 μm size fraction) with increasing distance from the Aley carbonatite. Yellow star-fenite, carbonatite, and Ospika diatreme boulders. Green arrow-landslides. A thick layer of overburden is located downhill of the Aley carbonatite. Legend for geology is the same as in Figure 2. For location see yellow markers (A-B-C) on Figure 2. Error bars based on average 2σ values determined from multiple analyses of standards by pXRF (Luck and Simandl, 2014).

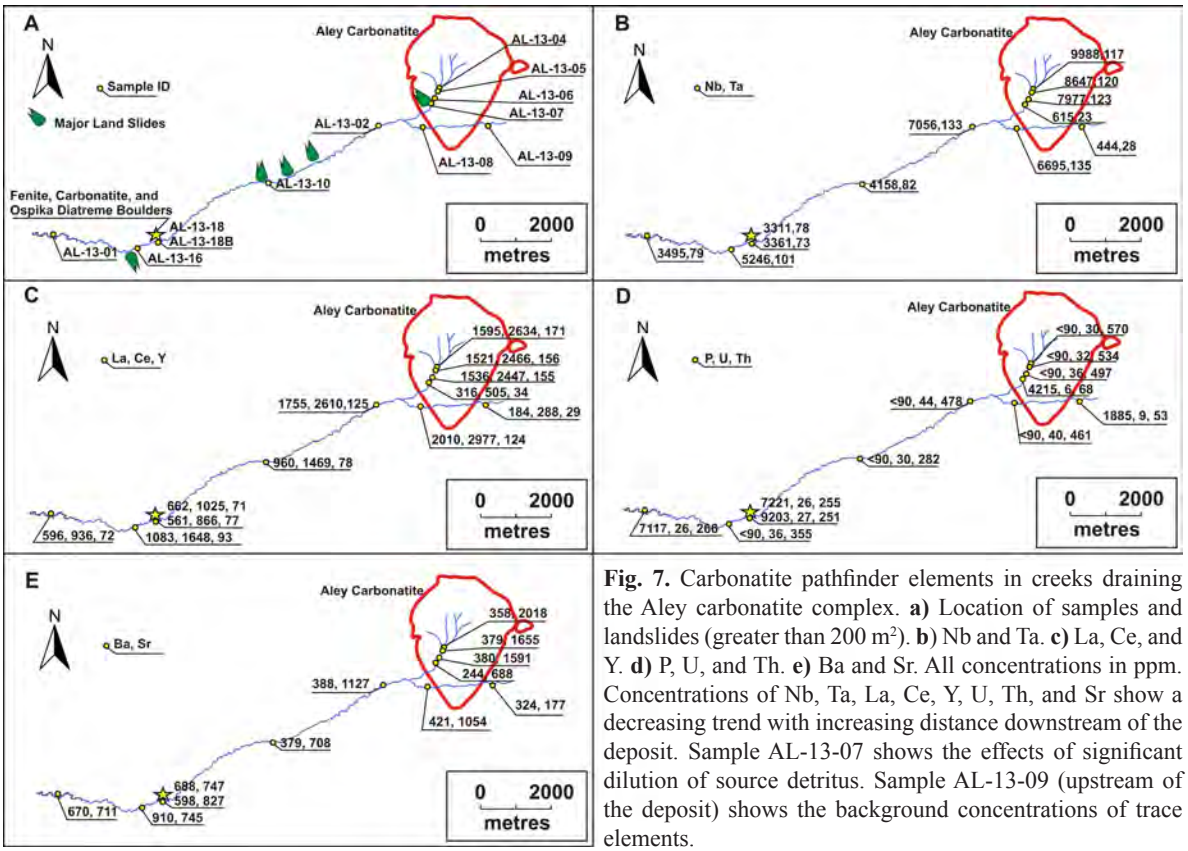

Fig. 7. Carbonatite pathfinder elements in creeks draining the Aley carbonatite complex. **a)** Location of samples and landslides (greater than 200 m^2). **b**) Nb and Ta. **c)** La, Ce, and Y. **d)** P, U, and Th. **e)** Ba and Sr. All concentrations in ppm. Concentrations of Nb, Ta, La, Ce, Y, U, Th, and Sr show a decreasing trend with increasing distance downstream of the deposit. Sample AL-13-07 shows the effects of significant dilution of source detritus. Sample AL-13-09 (upstream of the deposit) shows the background concentrations of trace elements.

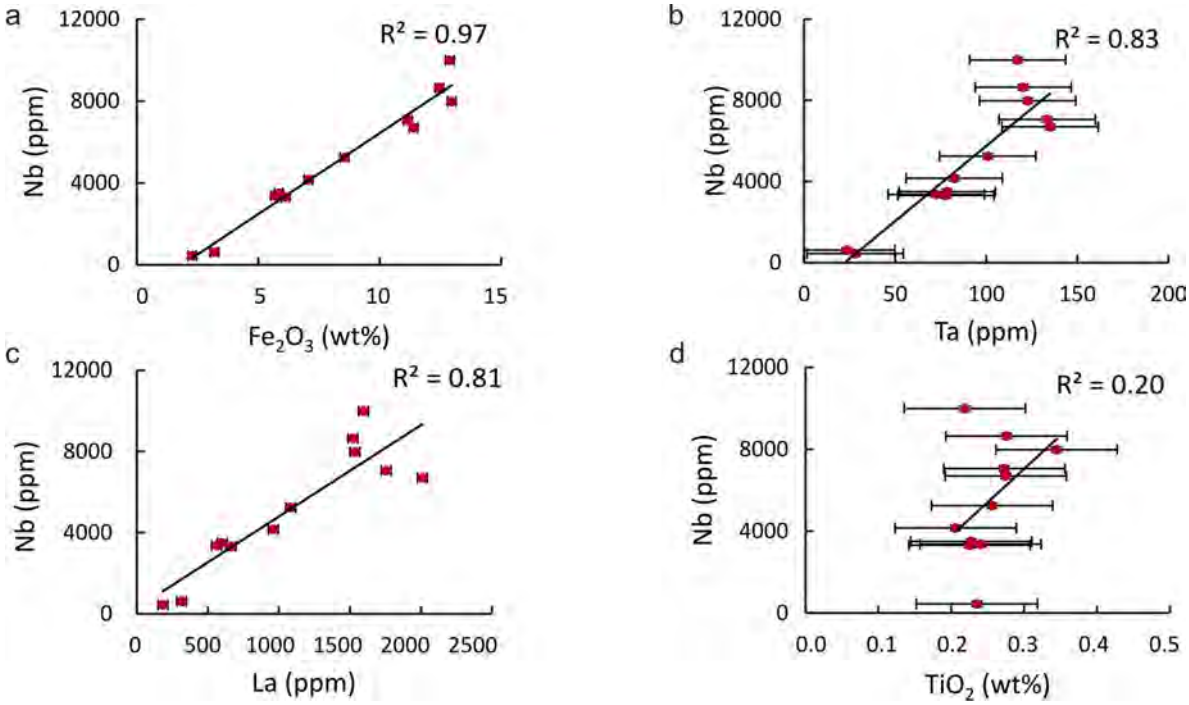

Fig. 8. Correlations between concentrations of **a)** Nb and Fe_2O_3. **b)** Nb and Ta. **c)** Nb and La. **d)** Nb and TiO_2. Error bars based on average 2σ values determined from multiple analyses of standards by pXRF (Luck and Simandl, 2014).

Table 2. Relative concentrations of major and trace element analysed by factory-calibrated pXRF. Samples are listed in order of increasing distance downstream of the deposit. Concentrations in ppm excepted were otherwise indicated. The data are internally consistent but have not been recalibrated as described in Simandl et al. (2013b) to improve accuracy by correcting for matrix effects and biases. Based on strong positive correlation between 11 U and 15 Th pXRF, and corresponding LMB-ICPMS analyses of stream sediments from Aley, Lonnie, and Wicheeda (unpublished) processed in exactly the same manner as those in the present study, systematic overestimation of U and Th, of the order of 35% and 90% respectively, is expected. [a]Total Fe as ferric oxide (Fe_2O_3).

Sample	Size Fraction (mm)	Nb	Ta	Y	La	Ce	Nd	Pr	Ba	Sr	P	U	Th	% Fe_2O_3[a]	% CaO
AL-13-09	+0.125	444	28	29	184	288	351	188	324	177	1885	9	53	2.28	10.94
AL-13-04	+0.125	9988	117	171	1595	2634	1579	661	358	2018	<90	30	570	12.88	29.34
AL-13-05	+0.125	8647	120	156	1521	2466	1453	614	379	1655	<90	32	534	12.45	27.84
AL-13-06	+0.125	7977	123	155	1536	2447	1443	623	380	1591	<90	36	497	12.96	27.06
AL-13-07	+0.125	615	23	34	316	505	580	289	244	688	4215	6	68	3.2	26.06
AL-13-08	+0.125	6695	135	124	2010	2977	1421	599	421	1054	<90	40	461	11.39	22.43
AL-13-02	+4.00	728	7	36	304	451	607	303	385	934	4475	6	63	3.32	31.84
	+2.00	585	<7	34	252	410	608	311	282	842	2788	4	70	4.03	29.99
	+1.00	2205	65	60	545	833	777	377	297	822	5983	16	255	7.75	28.55
	+0.500	5056	128	85	946	1402	1078	498	342	826	2894	60	451	15.06	25.42
	+0.250	7283	167	118	1274	1949	1276	561	370	1016	<90	62	549	15.24	24.36
	+0.125	7056	133	125	1755	2610	1347	571	388	1127	<90	44	478	11.16	23.75
	+0.063	2429	48	71	1048	1552	827	368	374	900	9412	18	192	4.63	21.83
	-0.063	530	<7	40	446	659	557	270	353	710	2042	5	67	3.34	22.48
AL-13-10	+0.125	4157	82	78	960	1469	870	390	379	708	<90	30	282	7.06	17.36
AL-13-18	+4.00	15	<7	14	166	269	442	254	427	545	560	<1	9	1.6	28.42
	+2.00	24	<7	15	122	194	414	225	516	349	<90	1	12	1.68	25.33
	+1.00	55	<7	16	128	209	387	219	588	352	<90	2	12	1.89	23.22
	+0.500	184	<7	20	159	266	403	196	574	375	<90	2	28	2.13	22.39
	+0.250	971	30	36	232	370	425	230	538	531	2292	9	99	3.34	21.6
	+0.125	3311	78	71	662	1025	721	355	688	747	7221	26	255	6.13	21.56
	+0.063	2250	44	62	813	1220	691	319	743	589	5224	16	177	4.44	19.7
	-0.063	321	<7	30	273	429	408	212	552	433	<90	6	45	3.13	20.6
AL-13-18B	+4.00	1142	<7	21	71	129	147	81	141	519	2264	3	71	1.31	30.58
	+2.00	67	<7	17	73	115	167	103	377	402	104	2	13	1.86	27.86
	+1.00	142	<7	18	87	145	191	104	427	393	260	1	22	1.91	25.69
	+0.500	431	<7	24	117	185	156	81	416	401	1636	4	47	2.46	23.57
	+0.250	1412	28	42	194	302	205	108	426	583	5036	11	129	3.75	23.16
	+0.125	3361	73	77	561	866	542	259	598	827	9203	27	251	5.69	23.24
	+0.063	3047	48	77	813	1208	458	193	604	703	5800	21	217	4.7	22.26
	-0.063	633	<7	36	416	614	396	187	552	491	453	9	68	2.82	23.8
AL-13-16	+0.125	5246	101	93	1083	1648	1028	470	910	745	<90	36	355	8.55	20.98
AL-13-01	+0.125	3495	79	72	596	936	724	346	670	711	7117	26	266	5.84	21.97

celestite solid solution. Sr is commonly a minor constituent of aragonite and calcite and is found in higher concentrations in REE-bearing carbonates, fluorocarbonates, and strontianite. Ba is also common in some REE-bearing carbonates, fluorocarbonates, and barite. All these minerals were reported by Mäder (1986) from Aley deposit and/or associated dikes; however, barite input from non-carbonatite sources such as dolostones of Kechika and Skoki Formations is an alternative explanation.

Ongoing work using a Frantz isodynamic separator and modern laboratory methods such as EMP, LA-ICP-MS, and QEMSCAN, will provide quantitative information on the indicator mineral signature of the Aley carbonatite deposit. The use of QEMSCAN is favored over grain-picking because many potential carbonatite indicator minerals are difficult to identify under binocular microscope. The pXRF chemical analyses presented here will be compared to and calibrated against laboratory chemical analysis for major and trace elements in an attempt to confirm and better quantify our data.

7. Conclusion

Stream sediment geochemistry represents a valid exploration method for Aley type carbonatite deposits. Niobium, Ta, La, Ce, Pr, Nd, Y, Th, U, and Sr in combination with each other, or alone, are good pathfinder elements in stream sediments. The Ba signature of the Aley deposit, if present, is masked by barite derived from dolostones. As P is a light element, it has to be present in higher concentrations than the above elements to be a useful pathfinder. The + 125 μm size fraction of the stream sediments is a useful geochemical sampling media and the most promising candidate for study of carbonatite related indicator minerals using QEMSCAN methods. Based on this study and the mineralogy of the Aley deposit, pyrochlore, columbite-(Fe), and fersmite are expected to be useful indicators. Monazite, REE-bearing carbonates, and fluorocarbonates, and to some extent fersmite and apatite are also possible indicator minerals based on the mineralogy of the deposit and chemical composition of stream sediments. Factory-calibrated pXRF is a cost effective method for determining relative concentrations of key pathfinder elements, such as Ni, Ta, La, Ce, Y, Th, U, and Sr in stream sediments; however, without recalibration, depending on the element, analyses can be strongly biased (e.g. Th or U). Additional mineralogical studies using modern laboratory methods such as EMP, LA-ICP-MS, and QEMSCAN, are required to establish relative concentrations of indicator minerals in stream sediments with increasing distance from the carbonatite.

Acknowledgments

This project received funding and support from Targeted Geoscience Initiative 4 (2010-2015), a Natural Resources Canada program carried out under the auspices of the Geological Survey of Canada. Logistical and helicopter support by Taseko Mines Limited is greatly appreciated. Critical review by Pearce Luck (British Columbia Ministry of Energy and Mines), John Gravel (ACME Analytical Laboratories Ltd.), and Jeremy Crozier (Hunter Dickinson Inc.) greatly improved earlier versions of this manuscript. The authors would also like to thank Pearce Luck for his assistance with sample preparation and analyses.

References cited

Chung, C.J., and Crozier, J., 2008. Assessment Report on Diamond Drilling performed on the Aley Carbonatite Property: British Columbia Ministry of Energy, Mines, and Petroleum Resources, Assessment Report 30113, 194 p.

Colpron, M., and Nelson, J.L., 2011. A digital atlas of terranes for the northern Cordillera. British Columbia Ministry of Energy and Mines, British Columbia Geological Survey, GeoFile 2011-11.

Irish, E. J.W., 1970. Geology of the Halfway River map area, British Columbia. Geological Survey of Canada, Paper 69-11, 154 p.

Kressall, R., McLeish, D.F., and Crozier, J., 2010. The Aley Carbonatite Complex – Part II Petrogenesis of a Cordilleran Niobium Deposit. In: Simandl, G.J., and Lefebure, D.V. (Eds.), International Workshop on the Geology of Rare Metals, November 9-10, 2010, Victoria, Canada. Extended Abstracts Volume. British Columbia Ministry of Energy and Mines, British Columbia Geological Survey, Open File 2010-10, pp. 25-26.

Luck, P., and Simandl, G.J., 2014. Portable X-ray fluorescence in stream sediment chemistry and indicator mineral surveys, Lonnie carbonatite complex, Canada. In: Geological Fieldwork 2013, British Columbia Ministry of Energy and Mines, British Columbia Geological Survey Paper 2014-1, this volume.

Mackay, D.A.R., and Simandl, G.J., 2014. Portable x-ray fluorescence to optimize stream sediment chemistry and indicator mineral surveys, case 2: Carbonatite-hosted REE deposits, Wicheeda Lake, British Columbia, Canada. In: Geological Fieldwork 2013, British Columbia Ministry of Energy and Mines, British Columbia Geological Survey Paper 2014-1, this volume.

Mäder, U. K., 1986. The Aley Carbonatite Complex. Master of Science thesis, University of British Columbia, 176 p.

Mäder, U. K., 1987. The Aley carbonatite complex, Northern Rocky Mountains (94B/5), British Columbia. In: Geological Fieldwork 1986, British Columbia Ministry of Energy, Mines and Petroleum Resources, British Columbia Geological Survey Paper 1987-1, pp. 283-288.

Mariano, A.N., 1989a. Economic geology of rare earth minerals. In: Lipman B.R. and McKay G.A. (Eds.), Geochemistry and Mineralogy of Rare Earth Elements. Reviews in Mineralogy, 21, 309-338.

Mariano, A.N., 1989b. Nature of economic mineralization in carbonatites and related rocks. In: Bell, K. (Ed.) Carbonatites: Genesis and Evolution. Unwin Hyman, London, pp. 149-176.

Massey, J.W.H., McIntyre, D.G., Dejardins, P.J., and Cooney, R.T., 2005. Digital geology map of British Columbia. British Columbia Ministry of Energy, Mines and Petroleum Resources, British Columbia Geological Survey Open File 2005-2, DVD.

McLeish, D.F., Kressall, R., and Crozier, J., 2010. The Aley Carbonatite Complex – Part I Structural Evolution of a Cordilleran Niobium Deposit Mine. In: Simandl, G.J., and Lefebure, D.V. (Eds.), International Workshop on the Geology of Rare Metals, November 9-10, 2010, Victoria, Canada. Extended Abstracts Volume. British Columbia Ministry of Energy and Mines, British Columbia Geological Survey, Open File 2010-10, pp. 21-24.

McLeish, D.F., 2013. Structure, stratigraphy, and U-Pb ziron-titanite

geochronology of the Aley carbonatite complex, Northeast British Columbia: Evidence for Antler-aged orogenesis in the foreland belt of the Canadian cordillera. Master of Science thesis, University of Victoria, 131 p.

Millonig, L.J., Gerdes, A., and Groat, L.A., 2012. U-Th-Pb geochronology of meta-carbonatites and meta-alkaline rocks in the southern Canadian Cordillera: A geodynamic perspective. Lithos, 152, 202-217.

Nethery, B.T., 2007. Report of technical exploration and development – 2006 evaluation and exploration planning on the Aley Carbonatite property, Ospika River, BC (Omineca Mining District). British Columbia Ministry of Energy, Mines, and Petroleum Resources, Assessment Report 28733, 410 p.

Pell, J., 1994. Carbonatites, nepheline syenites, kimberlites and related rocks in British Columbia. British Columbia Ministry of Energy, Mines and Petroleum Resources, British Columbia Geological Survey, Bulletin 88, 136 p.

Pride, K.R., 1983. Geological Survey on the Aley Claims. British Columbia Ministry of Energy, Mines, and Petroleum Resources, Assessment Report 12018, 16 p.

Pride, K.R., 1987a. 1986 Year End report on the Aley Property: British Columbia Ministry of Energy, Mines, and Petroleum Resources, Assessment Report 15721, 69 p.

Pride, K.R., 1987b. 1986 Diamond Drilling Assessment Report: British Columbia Ministry of Energy, Mines, and Petroleum Resources, Assessment Report 16484, 59 p.

Pyle, L.J., and Barnes, C.R., 2001. Conodonts from the Kechika Formation and Road River Group (Lower to Upper Ordovician) of the Cassiar Terrane, northern British Columbia: Canadian Journal of Earth Sciences, 38, 1387–1401.

Robert, M., Lyons, E.M., Hardy, J.L., and Nethery, B.T., 2005. Report of technical exploration and development – trenching, sampling, metallurgical testing and evaluation on the Aley carbonatite property, Ospika River, BC (Omineca Mining District): British Columbia Ministry of Energy, Mines, and Petroleum Resources, Assessment Report 27991, 60 p.

Simandl, G.J., Prussin, E.A., and Brown, N., 2012. Specialty metals in Canada. British Columbia Ministry of Energy and Mines, British Columbia Geological Survey, Open File 2012-7, 48 p.

Simandl, G.J., Reid, H.M., and Ferri, F., 2013a. Geological setting of the Lonnie niobium deposit, British Columbia, Canada. In: Geological Fieldwork 2012, British Columbia Ministry of Energy, Mines and Natural Gas, British Columbia Geological Survey Paper 2013-1, pp. 127-138.

Simandl, G.J., Fajber, R., Paradis, S., and Simandl, L.J., 2013b. Exploration for sedimentary phosphate (±REE) deposits using handheld XRF – An orientation survey. Geochemistry: Exploration, Environment, Analysis. http://dx.doi.org/10.1144/geochem2012-180. Available online.

Tantalum-Niobium International Study Center, 2013. Niobium - Raw Materials and Processing. <http://tanb.org/niobium> Accessed July 17, 2013.

Taseko Mines Limited, 2013. Aley Niobium Project; measured and indicated resources. <http://www.tasekomines.com/aley/ID539906> Accessed Nov 5, 2013.

Woolley, A.R., and Kjarsgaard, B.A., 2008. Paragenetic Types of Carbonatite as Indicated by the Diversity and Relative Abundances of Associated Silicate Rocks: Evidence from a Global Database. The Canadian Mineralogist, 46, 741-752.